PHILOSOPHICAL TRANSACTIONS OF THE ROYAL SOCIETY A
MATHEMATICAL, PHYSICAL & ENGINEERING SCIENCES

Melt Geometry, Movement and Crystallization, in Relation to Mantle Dykes, Veins and Metasomatism

B. Harte, R. H. Hunter and P. D. Kinny

Phil. Trans. R. Soc. Lond. A 1993 **342**, 1-21
doi: 10.1098/rsta.1993.0001

Melt geometry, movement and crystallization, in relation to mantle dykes, veins and metasomatism

By B. Harte[1], R. H. Hunter[2] and P. D. Kinny[1]

[1] Department of Geology and Geophysics, University of Edinburgh, Grant Institute,
West Mains Road, Edinburgh EH9 3JW, U.K.
[2] Department of Earth Sciences, University of Liverpool, P.O. Box 147,
Liverpool L69 3BX, U.K.

Consideration of theoretical, experimental and natural rock data show that basic-ultrabasic melt will disperse along mineral grain edges in olivine-rich mantle rock and thereby form a connected three-dimensional network throughout the rock even when present in only small (less than 1 %) volumes. The viscosity of such melts will also allow small (less than 1–5 %) volumes to move on appropriate geological timescales as a result of gravity-driven compaction. These features mean that small volume basic-ultrabasic melts are capable of infiltrating and metasomatizing mantle peridotites.

Modally metasomatized mantle xenoliths are commonly closely associated with an array of dyke-like and vein injection phenomena. Textural, structural and modal characteristics of a wide array of mantle dykes, veins and metasomatic rocks suggest that such rocks have certain features in common with cumulates, and might usefully be distinguished as *dyke cumulates* and *metasomatic infill cumulates*. They represent partial crystal precipitates from melt flowing along channelways or pervasively through peridotite, and their bulk rock compositions provide poor guides to actual mantle melt compositions. The crystallization of the minerals in dykes/veins/metasomites causes differentiation of the melt by crystal fractionation processes, but at the same time the melt may maintain equilibrium with host rock phases (e.g. olivine) and chromatographic column or percolation effects will control the range of transport of different chemical components by the melt. These combined processes are referred to as *percolative fractional crystallization*.

Data on the actual trace element compositions of melt in equilibrium with the minerals of mantle dykes/veins/metasomites are calculated from trace element analyses of the minerals by using partition coefficients. For a wide variety of metasomatic suites, the calculated melt compositions show a progression of trace element abundances from ones similar to primitive asthenospheric OIB-like compositions towards more incompatible element enriched compositions. Thus they support the hypothesis that fractional crystallization and percolative fractional crystallization processes operating upon initial primitive asthenospheric melts may yield melt compositions matching those necessary for wide varieties of mantle metasomatism. The differentiation of the melts and evolution of the metasomatic rocks proceed together. No evidence for the involvement of volatile-rich fluids distinct from melts has been found. The trace element compositions of many kimberlitic and lamproitic melts may also arise by processes of percolative fractional crystallization of initially primitive melts with OIB-like trace element compositions, as a result of flow through mantle peridotite.

Phil. Trans. R. Soc. Lond. A (1993) **342**, 1–21

Printed in Great Britain

1

Vol. 342. A (15 January 1993)

1. Introduction

This paper aims to consider the behaviour of basic-ultrabasic silicate melts in the mantle, and how they are related to the formation of metasomatic rocks and alkalic igneous rocks in the mantle lithosphere. The association in the mantle of modally metasomatized rocks with dykes and veins indicative of melt injection is emphasized. Particular attention is given to the way in which the crystallization of metasomatic minerals may be linked with the chemical evolution of melts injecting and percolating through peridotite, so that continuous varieties of both metasomatized rocks and melts responsible for one another may be formed. Evidence for these continua of variations of metasomatic rocks and associated melts is given by both petrographic and trace element data. The suggestions put forward are dependent upon the ability of basic and ultrabasic melts to move through peridotite matrices even when present in small volumes (less than 1–5%). The evidence relating to this, from theoretical and experimental standpoints as well as information from natural rocks (especially cumulates), is summarized in §2.

2. Melt geometry and melt mobility: theory, experiment and natural rock textures

The principles governing the shape of mineral grains and pores filled with fluids (including melts) in an aggregate of phases are well understood (Smith 1948; Voll 1960; Beere 1975; Kingery *et al.* 1976), and their importance in controlling melt and other fluid distribution in rocks has been the focus of much recent attention (Bulau *et al.* 1979; McKenzie 1984; Watson & Brennan 1987; Cheadle 1989; and papers quoted in table 1).

In simple terms the important question is whether small amounts of melt will tend to disperse along grain edges (as in figure 1*a*), or form isolated pockets (as in figure 1*b*). Under conditions of textural equilibrium, the melt distribution is controlled by the relative surface tension (or interfacial energy) of the interfaces of melt against solid by comparison with the solid–solid interfaces. These relative interfacial energies determine the geometrical relations of the melt pores with the solid grains, and are most simply expressed in terms of the dihedral angle formed by a melt pool in contact with two solid grains.

If the dihedral angle for melt between minerals is less than 60°, the melt disperses to form curved prismatic channels along the triple junctions between mineral grains (figure 1*a*). This means that the melt forms a continuously connected phase throughout the rock even if the melt is present in only vanishingly small amounts. Where the melt dihedral angle is more than 60°, small melt volumes will form isolated pores at grain corners and edges as in figure 1*b*. In this situation the establishment of continuous connection (connectivity) for the whole melt fraction depends on increasing the proportion of melt in the system until the pores of figure 1*b* meet one another. Figure 1*c* shows the dependence of melt connectivity on melt volume fraction and dihedral angle; with greater amounts of melt being necessary to establish connectivity as the dihedral angle increases. Where several solid phases are present, differences in dihedral angle may result in connectivity of melt being established between certain phases but not others (Toramaru & Fujii 1986).

Table 1 (after Cheadle 1989) lists experimentally determined dihedral angles for melts and solids of current interest. Most of the experiments have been done with

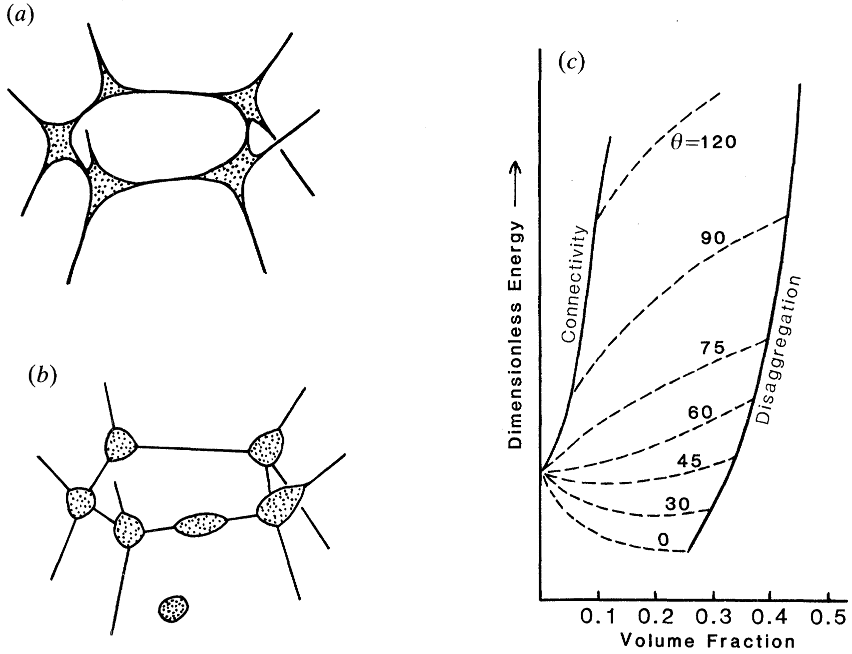

Figure 1. Textural and distribution relationships for a fluid phase. (*a*), (*b*) Melt pore shapes (dotted) in a three-dimensional aggregate of mineral grains for dihedral angles respectively below and above 60°. In (*a*) the melt extends along the grain edges between mineral grains. In (*b*) it forms isolated pools on grain edges or faces. (*c*) The volume fractions of melt necessary for melt 'connectivity' (continuous porosity) and 'disaggregation' (solid grains no longer in continuous contact) with various dihedral angles (after Beere 1975). θ is the dihedral angle.

basaltic melt and some contain H_2O and/or CO_2. Although there is some variation, it is clear, at least for olivine and probably orthopyroxene matrices, which dominate mantle rocks, that the dihedral angles for basaltic, komatiitic and carbonatitic melts are less than 60° and probably mainly in the range 25–40°. These data indicate that even very small melt fractions in the mantle should show connectivity and readily disperse through the rocks.

The formation of a connected three-dimensional melt network facilitates the relative upward movement of the melt with respect to its solid matrix under gravity. The length and timescales for gravity-driven compaction (McKenzie 1984, 1985) depend principally upon the material properties of the system: matrix and melt viscosities, melt density, and the permeability (which depends on dihedral angle; see Cheadle 1989). When the partly molten region is large in comparison to the compaction length, as it is in partly molten mantle, the compaction timescale is largely a function of melt viscosity. Basaltic melts (viscosity greater than 1 Pa s) will only separate from their matrix on reasonable geological timescales, if the melt fraction is greater than 1%; volatile-rich melts such as carbonatites with viscosities of *ca.* 10^{-1} Pa s will separate with melt volumes as low as 0.1% (O'Nions & McKenzie 1988; Hunter & McKenzie 1989).

The widespread mobility of mantle melt fractions of around 1% or less is clearly significant, because of its effect in concentrating and redistributing the incompatible elements which preferentially dissolve in the melt (McKenzie 1984, 1989). In basalt petrogenesis it provides a mechanism for small volumes of melt to extract

Table 1. *Summary of experimentally determined solid–solid–melt dihedral angles*

(ol, olivine; opx, orthopyroxene; cpx, clinopyroxene; ga, garnet; am, amphibole; pl, plagioclase; bi, biotite; af, alkali feldspar; qz, quartz; bas and, basaltic andesite; alk bas, alkali basalt.)

solid phase contact	melt composition	pressure (GPa)	temp. °C	dihedral angle	ref.[a]
ol–ol	basalt	1.0	1240	47	1
ol–ol	basalt	1.0	1230	22–35	2
ol–ol	basalt	1.0	1316	20–27	2
ol–ol	basalt	1.0	1360	21–26	2
ol–ol	basalt	1.5	1316	23–27	2
ol–ol	basalt	2.0	1316	29–38	2
ol–ol	basalt	2.0	1350	25–39	3
ol–ol	basalt	1.0	1300	49	4
ol–ol	basalt	1.5	1250	41	5
ol–ol	komatiite	0.0001	1400	32	6
ol–ol	alk bas	0.8	1250	46	6
ol–ol	basalt	0.3	1050	45	7
ol–ol	basalt	0.3	1255	43	7
ol–ol	komatiite	0.0001	1450	29–33	8
ol–ol	carbonate	3.0	1290–950	28	9
ol–opx	basalt	2.0	1350	24–40	3
ol–opx	basalt	1.5	1250	59	5
ol–opx	carbonate	3.0	1290–950	< 60	9
ol–ga	carbonate	3.0	1290–950	< 60	9
ol–am	bas and	0.8	1050	38	10
opx–opx	basalt	1.5	1250	52	5
opx–opx	basalt	1.0	1250	20–23	3
opx–opx	basalt	1.5	1350	29–34	3
opx–opx	basalt	2.0	1350	36–41	3
opx–opx	basalt	2.5	1350	33–40	3
am–am	bas and	0.8	1050	33	10
am–pl	bas and	0.8	1050	54	10
pl–pl	bas and	0.8	1050	60	10
bi–bi	silicic	1.2	1050	30	11
af–af	felsic	1.0	1000	44	12
af–qa	felsic	1.0	1000	49	12
qz–qz	felsic	1.0	1000	59	12

[a] References: (1) Waff & Bulau 1979. (2) Bulau 1982. (3) von Bargen & Waff 1988. (4) Toramaru & Fujii 1965. (5) Fujii *et al.* 1986. (6) Jurewicz & Jurewicz 1986. (7) Riley & Kohlstedt 1991. (8) Walker *et al.* 1988. (9) Hunter & McKenzie 1989. (10) Vincenzi *et al.* 1988. (11) Laporte 1988. (12) Jurewicz & Watson 1985. Based on a compilation by Cheadle (1989).

incompatible elements from a large volume of mantle. It also has application to many aspects of mantle metasomatism (Bailey 1982; Harte 1983; Menzies 1983) because it means that small volume melts can establish connectivity and move through rocks in a manner similar to that often envisaged for hydrous or other metasomatizing fluids. Even when relatively static, the dispersed and connected melt will provide a relatively fast transport medium for movement of material by diffusion compared to lattice diffusion through mineral matrices. Thus many mantle metasomatic and enrichment phenomena, which have been previously attributed to volatile-like fluids may potentially be products of infiltration by small-volume melts (Harte 1987). Indeed, where melts are present, metasomatism should be commonplace, since surface tension and gravity forces will cause melts to move along

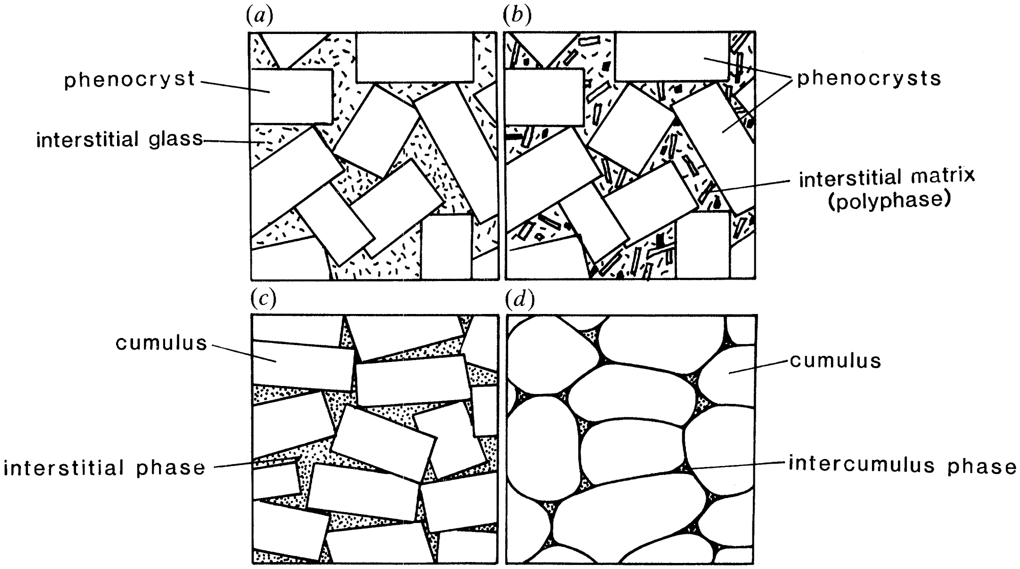

Figure 2. Schematic illustrations of textures in igneous rocks. (*a*), (*b*) Euhedral shapes of phenocrysts within a matrix whose overall shape mimics that of the pre-existing melt, which has been quenched to a glass in (*a*), and consists of a rapidly cooled aggregate of fine crystals in (*b*). (*c*) Typical cumulate texture with a cumulus mineral (whose euhedral-subhedral shape reflects growth within melt) and a substantial volume of intercumulus space occupied by only one other mineral. (*d*) A stage in the progression from (*c*) towards a monomineralic cumulate, with the cumulus mineral grains having substantial impingement upon one another and now showing granuloblastic (polygonal-granoblastic) shapes whilst the intercumulus volume is severely reduced, but still consists of only one phase.

grain edges in very small volumes and affect compositional alteration, without necessarily causing any obvious petrographic change.

In considering the theoretical and experimental evidence summarized above, a legitimate question has to concern the extent to which natural situations involving melt achieve local textural equilibrium and hence the predicted pore-system microgeometries. Consideration of this also raises important questions of how former melt is recognised once crystallization occurs, and to what extent localized crystallization products of the melt reflect its bulk composition.

Typical textures in igneous rocks, which clearly preserve evidence of former melt geometry, are often not symptomatic of textural equilibrium. The euhedral shapes of crystals preserved in a quenched glass or rapidly chilled fine-grained crystalline matrix (figures 2*a*, *b*), are a product of crystal growth mechanisms in melt rather than textural equilibration. In many basalts and dolerites such intersertal and interstitial textures are common, and where the matrix is glass or comprises many phases it probably approximates to the host melt composition. In other cases, as in many gabbros and cumulates, a single mineral forms the interstitial matrix phase (figure 2*c*). This single interstitial or intercumulus phase is typically one of the common silicate minerals and it is evident that it can in no way provide a reasonable estimate of the consanguinous melt composition. Yet the texture (figure 2*c*) is essentially similar to that where the interstitial matrix is glass or a polyphase aggregate (figure 2*a*, *b*), and it is evident in all cases that the interstitial matrix has taken on the melt shape and can be loosely described as a *melt pseudomorph*. The melt shape assumed by the interstitial/intercumulus phase is not a pseudomorph of the melt at one instant of time, but is a relict of melt shape formed over an interval of time during which cumulus and intercumulus phases were growing.

The texture highlighted in figure 2*c*, where a single interstitial phase pseudomorphs melt geometry is common over a wide variety of situations (Hunter 1987; Harte *et al.* 1991 *a*). Clearly during the crystallization of the single interstitial/intercumulus phase, its chemical components must have become concentrated in the particular intercumulus volumes concerned, while other melt components, destined for other phases, migrated elsewhere. Such migration must have remained efficient even with very small melt fractions and will clearly have been facilitated by the connectivity of the melt along grain edges predicted by the theoretical and experimental data discussed above. Particular evidence of such inter-connected porosity at small melt volumes is seen in rock textures where the interstitial material forming several intercumulus pools is a single crystal (oikocryst) even though such pools appear disconnected in two dimensions. The transport of melt components through the intercumulus volume will also be considerably aided by relative movement (two-phase flow) of melt and crystalline material, which may be expected to occur by gravity-driven compaction in situations such as typical layered cumulate bodies and the mantle (McKenzie 1984, 1989; Hunter 1987).

In seeking analogies with mantle conditions, basic-ultrabasic layered cumulate bodies provide excellent examples of situations where we may observe minerals and melts kept at high temperatures for relatively long periods of time, with melt percolating through a crystalline matrix. Cumulates also give evidence of a variety of textures formed under differing conditions of porosity (melt fraction), including situations where the amount of melt is very small. Monomineralic cumulates represent an extreme example of rocks where efficient transport of melt components, even at very small melt fractions, has allowed only one phase to form. In cumulates, progression towards very low abundances of intercumulus minerals, commonly goes hand-in-hand with progression towards textural equilibrium, as illustrated by the textures of figure 2*c* and *d* and the type monomineralic accumulates of Wager *et al.* (1960). The changes in grain shape associated with this progression and the compaction accompanying it may be affected by a number of mechanisms (e.g. solution-reprecipitation, diffusion, dislocation creep), but the result, under the usual conditions of little crystalline strain, is always to produce a lower energy grain geometry. This progression towards textural equilibration will, therefore, ensure that the melt maintains an inter-connected porosity as the melt fraction becomes small, and thereby will allow migration of melt components even at very small melt fractions.

The percolation of intercumulus melt by compaction in large basic and ultrabasic intrusions is likely to be applicable to the movement of small fractions (1–5%) of melt through partly molten regions within the mantle. It is notable that just as textural evidence of thorough-going textural equilibrium throughout large rock volumes is limited in layered cumulate bodies, so it is in the mantle. Many of the common coarse mantle xenoliths show relatively poorly developed granuloblastic textures and therefore have only a moderate degree of textural equilibrium between mineral grains (Harte 1977). Thus for melt connectivity and mobility to have been established in such rocks, there can only have been localized textural equilibrium along grain edges as seen in some layered cumulates. Specific evidence supporting this is seen in the wallrocks to many mantle dyke-like bodies (Wilshire & Shervais

PHILOSOPHICAL TRANSACTIONS OF THE ROYAL SOCIETY A MATHEMATICAL, PHYSICAL & ENGINEERING SCIENCES

Table 2. *Modal metasomatic associations*

erupting host	principal metasomatic mineral in peridotites	associated dykes and veins at depth
(1) highly alkaline volcanics in continental rifts	*clinopyroxene, biotite, amphibole* titanomagnetite, sphene, apatite (calcite, feldspar)	*clinopyroxenites* (with apatite and titanomagnetite)
(2) alkali basalt–basanite–nephelinite series	*kaersutite/pargasite, biotite*, apatite, ilmenite. clinopyroxene	Al–augite wehrlite–pyroxenite dykes, amphibole–mica (lherzite) veins
(3) kimberlite	*biotite, K-richterite, clinopyroxene,* K–Ba–titanates, ilmenite, rutile, apatite, zircon. (*Marid type*)	MARID suite dykes and biotite–richterite veins
(4) kimberlite	*ilmenite, rutile, biotite, sulphides,* clinopyroxene, garnet (*Matsoku type*)	opx- and cpx-rich dykes and veins, (with garnet and IRPS minerals)
(5) kimberlite	*edenite, biotite,* clinopyroxene (*Jagersfontein type*)	rare zones rich in cpx and/or amphibole and/or biotite

1975; Irving 1980; Harte *et al.* 1987), where there is chemical compositional evidence of melt infiltration, despite a lack of textural equilibrium amongst the crystalline phases, or any petrographic evidence of the passage of the melt. Recently, Matthews *et al.* (1992) have provided further evidence from the occurrence of healed fractures in garnets in such wallrocks, that melt must have infiltrated these rocks despite the fact that the petrographic textures show only a moderate approach to textural equilibrium between mineral grains.

3. Mantle dykes, veins and metasomatic rocks: xenolith petrography

(*a*) *Associations of dyke, vein and modal metasomatic rocks*

The occurrence of metasomatism in mantle rocks is now widely accepted and there is considerable evidence to show that such phenomena are in situ mantle processes, and not merely the result of alteration during and/or following eruption (Harte 1983, 1987; Menzies 1983; Dawson, 1984). Metasomatism may take place with or without changes in the petrography of the rocks, and where such changes occur they do so both by introduction of new phases such as biotite, amphibole, ilmenite, rutile and apatite, and by changes in the proportions and compositions of those typical peridotite–pyroxenite minerals originally present (i.e. olivine, pyroxenes and garnet). Such modal metasomatism may be classified according to the nature of the minerals occurring and their associations, and the principal types of metasomatism found in mantle xenoliths are summarised in table 2 (after Harte & Hawkesworth 1989).

As indicated in table 2, mantle rocks exhibiting modal metasomatic mineralogies are commonly found alongside others bearing direct evidence of mantle melt/fluid interaction in the form of intrusive dykes and veins, and it is important to consider these phenomena in conjunction (Gurney & Harte 1980; Harte 1983; Wilshire 1987). Thus we shall briefly review the variety of dyke and vein phenomena and their relation to modal metasomatic rocks.

The most widely reported phenomena providing evidence of intrusive sheet and vein-like bodies traversing mantle peridotite are from xenoliths erupted with alkali basalts. They show a wide range of characteristics with gradations towards the features seen in xenoliths from highly alkaline continental rifts (Menzies 1983; Lloyd 1987; Witt & Seck 1987). The fragmentary nature of the specimens retrieved from alkali basalts means that the overall relationships have to be pieced together. However, studies of composite xenoliths, and comparisons with relationships seen in alpine peridotite massifs, have made it possible to construct clear pictures of the dyke/vein relations to the country-rock peridotites, determine orders of intrusion, and suggest mechanisms of emplacement involving hydraulic fracturing (Wilshire & Pike 1975; Irving 1980; Wilshire *et al.* 1980; Nicolas & Jackson 1982; Wilshire & Shervais 1985). The dykes and veins in basalt-derived xenoliths vary widely in modal mineralogy, but are usually dominated by either clinopyroxene (typically Al–Ti–augite) or amphibole (kaersutite–pargasite) and as such may be relatively anhydrous or hydrous. The more abundant clinopyroxene-rich varieties form the Al–augite wehrlite–pyroxenite (or Type II) xenoliths (see reviews of Menzies 1983; Harte & Hawkesworth 1989), and there is a continuum of compositions between these and amphibole or amphibole–mica (lherzite) dominated veins (Wilshire & Trask 1971; Wilshire *et al.* 1980; Wilshire 1987), some of which carry substantial apatite (Wass *et al.* 1980). The full range of commonly occurring minerals is: clinopyroxene, orthopyroxene, olivine, amphibole, biotite, spinel, apatite, ilmenite and magnetite. Plagioclase may occur in lower pressure varieties, while there are also some garnet pyroxenite xenoliths which seem to be related (Frey 1980; Griffin *et al.* 1984). There are close counterparts to minerals of the Type II dykes/veins in the so-called megacryst minerals, which occur as xenocrysts in alkali basalt, and have been considered to represent phenocrysts from deep-seated magmas.

Dykes and veins are not so common in the kimberlite-sampled mantle material, but those that have been described show similar structural and textural features to the basalt-derived material, despite differences in mineralogy. Thus analogues of the basalt-derived lherzites are seen in veins rich in amphibole and mica, which have been extensively described traversing peridotite in xenoliths from the Kimberley area (Jones *et al.* 1982; Dawson 1987; Erlank *et al.* 1987). In these veins the amphibole is a K-richterite, and there is an association with a diverse suite of MARID intrusive sheets/dykes in kimberlites (table 2) consisting of widely variable proportions of MARID minerals (mica, amphibole, rutile, ilmenite, diopside), together with apatite, zircon and unusual titanates (Dawson & Smith 1977; Dawson 1987; Haggery 1983; Waters 1987). Similarities to the more anhydrous Type II dykes and veins from basalts are shown by the Matsoku xenolith suite (Harte *et al.* 1987). This includes dykes/sheets which show widely varying proportions of the common peridotite minerals (olivine, orthopyroxene, clinopyroxene, garnet) as well as *IRPS* minerals (ilmenite, rutile, phlogopite and sulphides), which are also prominent in associated metasomatic rocks. Similar metasomatic phenomena, where ilmenite is prominent, have been described from other kimberlites (Wyatt & Lawless 1984), and there are compositional links also between the Matsoku suite and the common Cr-poor megacryst suite in kimberlite (Harte *et al.* 1991*b*) and with the metasomatism affecting high-temperature deformed peridotites (Gurney & Harte 1980; Harte 1983). The Jagersfontein metasomatic suite, characterized by edenite and mica (table 2), shows the least evidence for dyke and vein structures (Field *et al.* 1989; Winterburn *et al.* 1990) though rare mica veins have been found (P. A. Winterburn, personal communication).

Examination of material from localities where both dyke/vein and modally

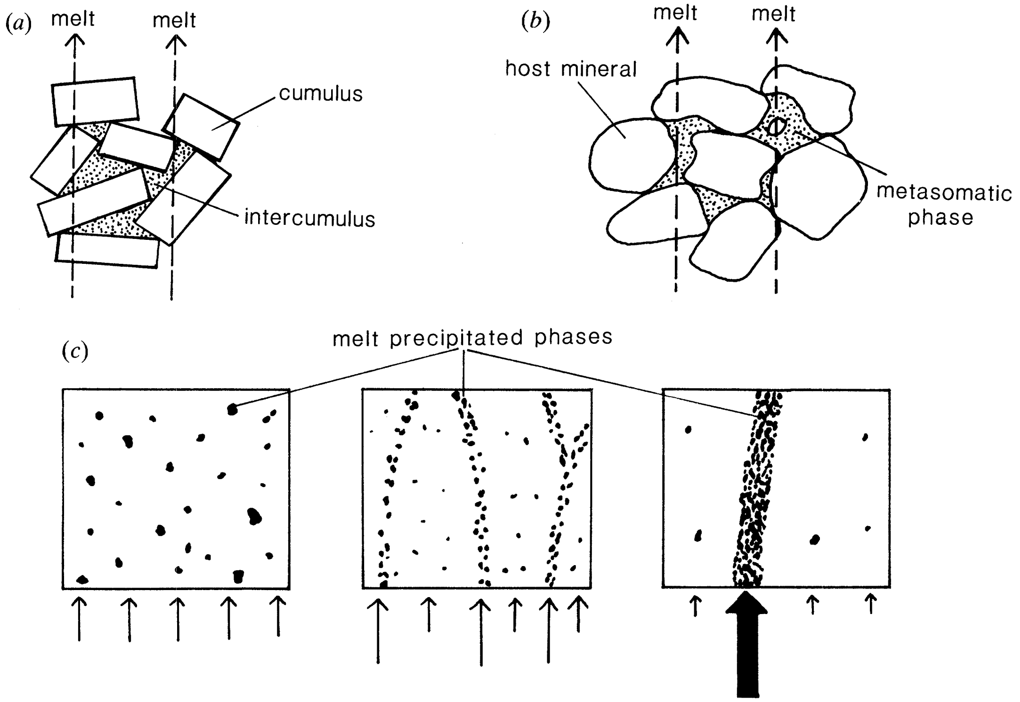

Figure 3. (*a*), (*b*) Comparison of the situations for normal cumulates and metasomatic infill cumulates. In both, a melt phase is percolating upwards, and in the former crystallizes the intercumulus phase which fills the original melt porosity between the gravity-settled cumulus crystals. In (*b*) the percolating melt deposits a metasomatic mineral phase in the melt porosity, which in this case lay within a grain network formed by host peridotite minerals. (*c*) The outlined boxes represent cross sections of peridotite within which minerals are being deposited from a melt flowing/percolating upwards; various degrees of channelizing of the melt flow are shown resulting in variations from pervasively metasomatized peridotite, through veined peridotite to dyke intruded peridotite. Arrows at bottom indicate relative variation in input of melt, which will vary over time as minerals are deposited by the melt.

metasomatized rocks are abundant, shows that these rock types appear to be very closely related. The evidence may be summarized as follows:

(*a*) The minerals introduced into modally metasomatized peridotites are commonly found in dykes and veins, where either they show similar chemical compositions or there are gradients in chemical compositions between peridotite and dyke/vein.

(*b*) A close spatial association may be visible in individual xenoliths (e.g. peridotites carrying veins are also often pervasively metasomatized with the widespread development of a vein mineral).

(*c*) Variations may be found from discrete dykes and veins to situations with more irregular concentrations of dyke/vein/metasomite minerals, to a completely dispersed distribution of dyke/vein/metasomatic phases (figure 3*c*).

(*d*) The dykes/veins from all the associations are extremely variable in modal composition, extending to virtually monomineralic rocks (e.g. clinopyroxenites, orthopyroxenites, amphibolitites, glimmerites), and these have their counterpart in wide modal variations in the metasomatized rocks (e.g. ‘peridotites’ containing abundant mica, or amphibole, or ilmenite).

(*e*) The host rock phases in metasomatized peridotites (e.g. olivine, pyroxenes, garnet) show changes in their chemical composition (e.g. Fe/Mg, Al/Cr) towards compositions found in the dykes/veins.

(b) *Textures and structures in dykes, veins and modal metasomatic rocks*

Both the dyke/vein and their associated modal metasomatic rocks show a wide variety of textures, which are reminiscent of the range of textures seen in cumulates, from ones clearly showing igneous textures to ones showing good solid–solid textural equilibrium. Thus in dykes, one may find euhedral/subhedral crystal shapes, interstitial and poikilitic/oikocrystic textures, and granuloblastic (polygonal granoblastic) textures (Wilshire & Shervais 1975; Frey & Prinz 1987; Harte *et al.* 1987; Harte & Matthews 1989). In the last type equant polygonal grains suggest a high degree of textural equilibrium, and are most common in monomineralic portions of the dykes, suggesting a parallel with accumulates. In some cases replacement textures suggest that multiple injections of melt/fluid have occurred along the dykes (Wilshire *et al.* 1980; Irving 1980).

In some cases in modal metasomatic rocks, there is also clear evidence of replacement of a pre-existing phase (usually olivine, orthopyroxene or clinopyroxene) by a metasomatic phase (usually amphibole or mica); (see Erlank *et al.* 1987, figs 6 to 8; Winterburn *et al.* 1990, fig. 2). Sometimes the metasomatic replacing phase has a dispersed poikilitic or oikocryst habit, which bears a close resemblance to the way the intercumulus phase in many cumulates shows crystallographic continuity across a series of interstitial spaces, and thereby provides evidence that the metasomatic phase crystallized from the melt/fluid. Occasionally, euhedral inclusions of olivine or orthopyroxene occur, within the metasomatic phases (Harte *et al.* 1987) and provide further evidence of crystallization from a melt. In other cases the metasomatic phases show a much closer approach to textural equilibrium characteristics, having smoothly curving grain boundaries and regular triple junctions. Such cases are interpreted as evidence that the metasomatic minerals reached textural equilibrium under near-solidus conditions as in the case of accumulates.

More particular evidence of the growth of metasomatic mineral aggregates from melt pools within peridotite is shown by ilmenite aggregates (see fig. 10, Harte *et al.* 1987) in the Matsoku peridotites (Harte & Matthews 1989). The ilmenites were found to have a broad and partly bimodal spectrum of dihedral angles against olivine and orthopyroxene: smaller angles (close to 60°) apparently matching those of melts, larger angles (near 100°) conforming to experimentally determined equilibrium angles for ilmenite-silicate textures (Matthews & Harte 1989). The Matsoku ilmenite aggregates are likened to the interstitial phase in many cumulates, originating by crystallization from melt pockets and retaining shape features which are partly those of the melts, while simultaneously moving towards textural equilibrium for the solid phases. The development of such features is considered to be dependent on the flow of melt through the rocks, which allows crystallization of only one phase while other melt components are carried away by the flowing melt (Harte & Matthews 1989).

In the dykes occurring with the various modal metasomatic associations it is quite common to find layering parallel to their walls (Irving 1980; Wilshire *et al.* 1980; Harte *et al.* 1975, 1987; Dawson & Smith 1977). Such layering has been attributed to magma flow and crystal plating on conduit walls, and although the overall features indicate more varied situations than crystal plating alone (Wilshire *et al.* 1980; Harte & Hunter 1986), it clearly indicates processes whereby crystals and melt become selectively separated.

(*c*) *Crystallization processes in dykes, veins and modal metasomatic rocks*

For all of the dyke/vein associations listed in table 2, an origin by silicate melt intrusion has been widely accepted for the larger dyke-like bodies, because of the involvement of a wide array of both anhydrous and hydrous minerals. However, for smaller vein-like bodies and for metasomatized rocks rich in hydrous phases, the nature and composition of the metasomatizing fluid is more debatable with many authors favouring hydrous volatile fluids (Menzies *et al.* 1987). We suggest that the continuum of wide variations in modal mineral proportions, both hydrous and anhydrous, in various dyke/vein/metasomite associations (table 2), provides no evidence for distinguishing ones which have crystallized from a hydrous fluid rather than a melt. Because of this and the fact that melts may yield both hydrous (e.g. amphibole-rich) and anhydrous (e.g. clinopyroxene-rich) precipitates, while non-molten fluids have limited element transport capabilities (Eggler 1987), we further suggest that the dyke/vein/metasomite rocks are in general melt-derived. Further evidence in support of the possibility that all dykes/veins/metasomites are melt-derived is given on the basis of the trace element data presented in the next section.

In considering the crystallization processes of the dyke/vein bodies, it is important to take into account the wide variations in mineral proportions found in closely related dykes/veins in all the associations described, coupled with the internal layering structures, and the similar range of textural features to those found in cumulates. All suggest that the dyke mineralogy is controlled by dynamic and kinetic factors of two-phase flow and crystallization. Under such circumstances, the crystal aggregates clearly do not represent bulk melt compositions, but are aggregates and residues deposited and left behind by the flowing melt. Thus the assemblages in the dykes and veins are analogous to layered intrusion cumulates in the sense that they represent crystal residues reflecting processes of crystal sorting, melt flow and percolation, and kinetic controls (e.g. nucleation and growth). At the same time they are certainly not simple products of crystal settling and for this reason, it is proposed to call them *dyke cumulates*. It is pertinent to note that their bulk trace element geochemistry is also similar to that of normal cumulates in reflecting the loss of incompatible components carried away with the melt (Frey & Prinz 1978; Irving 1980; Waters 1987).

Modal metasomatic rocks are envisaged as products of melt infiltration and injection, where, in comparison to the dyke and vein facies, the melt was more dispersed and percolating through a peridotite matrix (figure 3). In addition to any direct replacement reactions, the metasomatic phases are interpreted to have grown to fill the melt porosity (which might be less than 1.0% or up to about 30%) that existed when melt was flowing through the rocks, in similar manner to the way intercumulus material replaces space previously occupied by melt (figure 3). As the matrix in this instance is the host peridotite, the analogy to cumulates made here does not so much involve the cumulus crystals themselves as the intercumulus material, and for this reason we refer to the metasomatic rocks as *metasomatic infill cumulates* (figure 3). Note that the metasomatic phases infilling the melt porosity, may be both monomineralic and polymineralic, in a similar way to intercumulus material. Where percolation and transport processes combine with crystal nucleation processes to produce monomineralic metasomatic material, the effects upon bulk rock composition are much more striking, but the metasomatic material necessarily gives a poor guide to bulk melt composition.

In addition to the crystal deposition, infiltrating melts would be expected to react and equilibrate with the host peridotite, thereby causing an exchange of elements with the matrix crystalline phases according to chromatographic column and percolation principles (Hoffman 1973; McKenzie 1984; Navon & Stolper 1987; McKenzie & O'Nions 1991). The flowage of melt through the rocks, therefore, represents a complex process in total. On the one hand there is modification of the melt by interchange with the host rock according to a percolation exchange process. On the other hand the melt is changing as a result of precipitating and leaving behind the metasomatic phases, which is a type of crystal fractionation process. The combination of processes can thus be described as '*percolative fractional crystallization*'. The difference of this melt differentiation process to normal crystal fractionation is that the melt is maintaining at least partial equilibrium with the host rock phases it is percolating through. Maintenance of equilibrium with olivine, the most abundant and ubiquitous of host rock phases, is particularly to be expected and will mean the melt remains rich in compatible elements such as Ni and Co.

4. Use of trace element data on minerals from dykes and metasomatic rocks to determine mantle melt compositions

It is difficult to know the percentage of melt that may have been present at any one time in the metasomatized rocks, or the amount of melt that may have passed through the dykes/veins/metasomites and the extent to which equilibrium with host rock phases was maintained. Clearly the processes described above result in differentiation of the flowing and percolating melt, and leave the dyke, vein and metasomatic phases as residua. Thus bulk rock compositions for dykes/veins/metasomites will be no better guide to melt compositions than bulk cumulate rock compositions are to the melts responsible for them. To reconstruct melt compositions it is therefore imperative to use mineral compositions that coexisted with the melts and calculate the melt composition with the use of appropriate partition coefficients. This approach offers particular promise with trace elements.

The amount of mineral trace element data from xenoliths, as distinct from whole rock and major element data, that is available in the literature is quite small (see particularly Shimizu (1975) and Kramers *et al.* (1981) for kimberlite-derived peridotites and megacrysts; Kramers *et al.* (1983) for MARID related rocks; Wass *et al.* (1980), Irving & Frey (1984), Menzies *et al.* (1985) for basalt-derived xenoliths and megacrysts). Much of this data was compiled and reviewed by Menzies *et al.* (1987), who also calculated some melt compositions from them. Their compilations showed considerable similarities, with generally gradual variations in concentrations, between trace element distribution patterns for mineral phases derived from dykes, veins and metasomatic rocks as well as from megacrysts.

We have augmented these data with new analyses of clinopyroxene, amphibole, garnet and mica from the Matsoku, Jagersfontein and Eifel xenolith suites. The new data have been gathered by using the Cameca ims 4f ion microprobe at Edinburgh University. This technique consists of routine *in situ* SIMS analysis of various REE, LILE and HFSE derived from a 20–30 μm spot on the target mineral by bombardment with an 8–10 nA oxygen ion beam, and using a 100 eV energy offset to minimize isobaric spectral interferences (for analytical details see Matthews *et al.* (1992)). Elemental abundances are normalized against analyses of NBS610 glass, and validated by analyses of mineral standards. Detection limits for the REE range from 10 to 100 p.p.b. The full data-set will be published elsewhere.

Melt compositions have been calculated, from this new data and those already in the literature for clinopyroxenes and amphiboles, for the spectrum of dyke, vein and metasomatic rock associations given in table 2. The partition coefficients used are those adopted by McKenzie & O'Nions (1991), coupled with use of the same values for Y and Zr as for Ho and Hf respectively; together with the addition of a value of 0.5 for Ba between amphibole and melt based on Irving & Frey (1984), and a guessed one of 0.05 for Ba distribution between clinopyroxene and melt. Representative calculated melt compositions are shown in figure 4. These are normalized to chondritic abundances taken from Sun & McDonough (1989).

Figure 4*a* shows calculated melts coexisting with clinopyroxenes from dykes/veins/metasomatic rocks and a megacryst collected from kimberlite sources. Although LREE vary in concentration by an order of magnitude, the patterns show considerable regularity, and reveal a fanning array, with progressively increasing LREE-MREE away from the melt composition coexisting with the megacryst (MEGA 1600E). The megacryst melt composition has been shown to be consistent with that expected for a primitive asthenospheric OIB-like melt (Harte 1983; Jones 1987). Thus the progressive enrichment in LREE and MREE seen in the metasomatic melt compositions in figure 4*a* may be generated by progressive extraction of metasomatic phases (especially clinopyroxene, garnet and amphibole) from a primitive asthenospheric melt. The restricted enrichment in HREE seen in melts may be attributed to involvement of garnet, which coexists with all the clinopyroxenes/melts represented in figure 4*a* except for the MARID-type ones. Even for the MARID series rocks there is a close association with garnetiferous peridotites (Dawson 1987; Erlank *et al.* 1987), so that there may well have been little differentiation of the MARID melt away from compositions in equilibrium with garnet. It is also significant to note that much of the overall spectrum of compositions shown in figure 4*a* is represented by two metasomatized rocks from Jagersfontein (J13, rich in clinopyroxene and mica; J134, with edenitic amphibole) where there is evidence of progressive evolution from amphibole-free to amphibole-bearing rocks (Winterburn *et al.* 1990).

Figure 4*b* shows a similar set of trace element abundance patterns for calculated melts in equilibrium with clinopyroxenes from alkali basalt sources. The data shown were chosen to encompass the broad spectrum of compositions found in Type II dykes, metasomatic rocks and megacrysts, but data from type Type IA spinel lherzolite xenoliths were excluded since these have been linked to residua depleted by partial melting (Frey & Prinz 1978; Menzies *et al.* 1985). Given the variety of sources, the data show a strikingly limited range of compositions. The most enriched liquid composition is that calculated from clinopyroxenes in a set of amphibole and apatite-rich xenoliths described by Wass *et al.* (1980) as fractionates. Slopes of the melt REE patterns vary widely, resulting in crossovers in the MREE range, but the steeper slopes (and Ce/Ho for example) are notably similar to those calculated for melt coexisting with the kimberlite-derived megacryst of figure 4*a*. Evidence for garnetiferous precursors to basalt-derived peridotites has been noted (Nicolas 1986), and the variations in LREE/HREE in figure 4*b* may be linked to the extent to which melt differentiation has occurred in the presence or absence of garnet (cf. Menzies *et al.* 1987, p. 347). Allowing for this factor, the spectrum of melt compositions in figure 4*b* shows many similarities to that in figure 4*a*. Thus derivation of all these melt

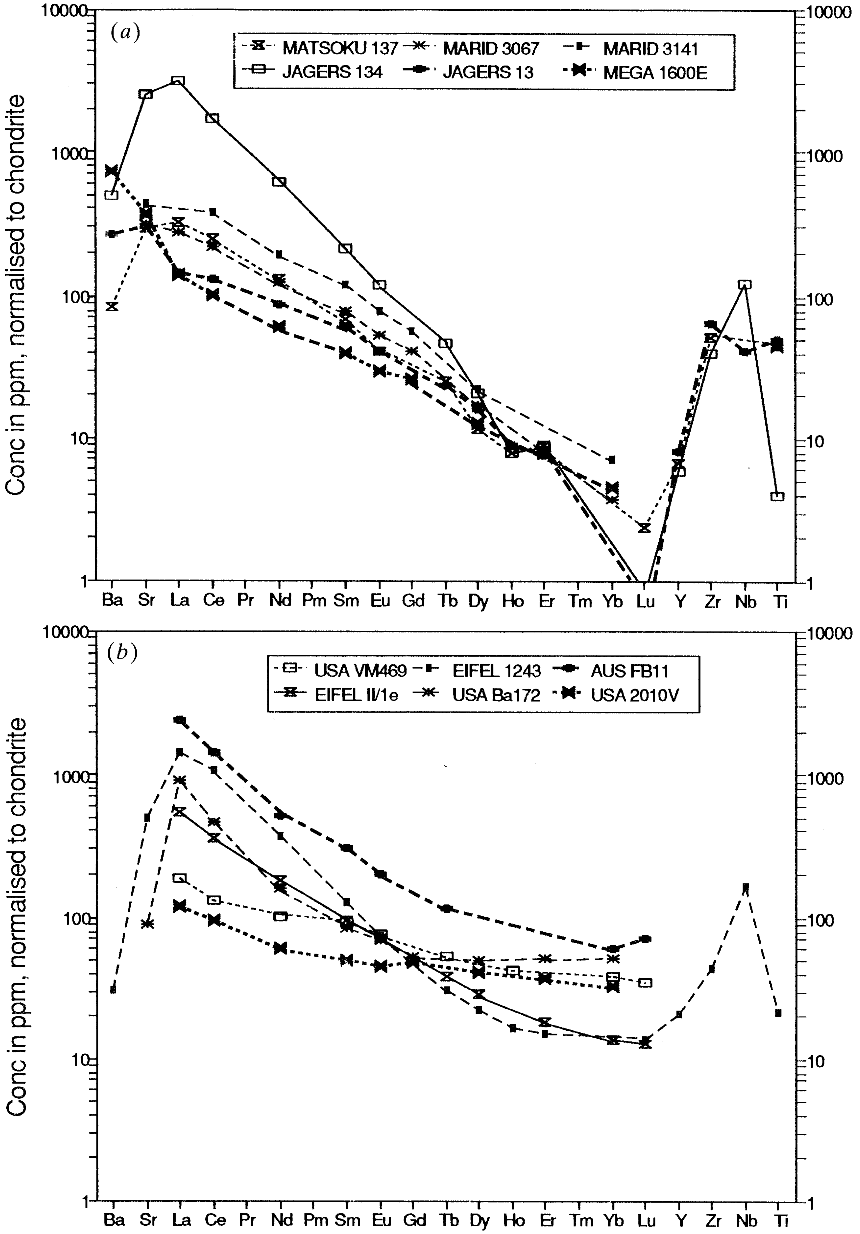

Figure 4*a*–*b*. For description see opposite.

compositions from similar source liquids of primitive OIB-like trace element characteristics, would be possible by a differentiation process such as percolative fractional crystallization (as described above).

Exactly the same features are shown by the melt compositions calculated from amphiboles from various dykes, veins, metasomites and megacrysts (figure 4*c*). The melts calculated from the kimberlite-derived amphiboles have relatively high LREE/HREE, similar to some of the basalt-derived compositions, e.g. Eifel, while other basalt-derived amphiboles yielded melt compositions with lower LREE/HREE.

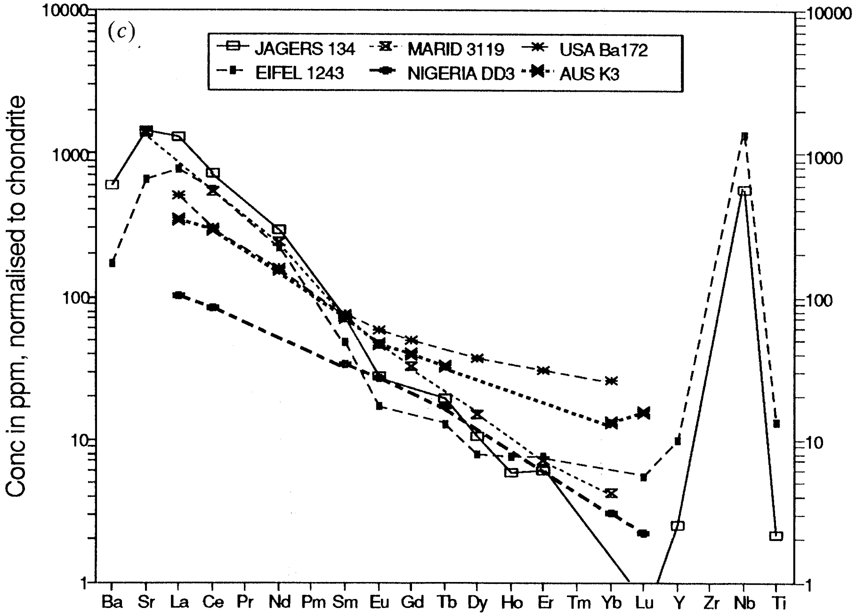

Figure 4. Melt compositions (chondrite normalized) coexisting with clinopyroxenes and amphiboles, calculated by using partition coefficients (see text). (*a*) Melts coexisting with clinopyroxenes from various kimberlite-derived metasomatic associations (Marid, Matsoku and Jagersfontein types; see table 2). In addition a Cr-poor megacryst composition has been used to calculate a melt composition (Mega 1600E) which is believed to be representative of primitive OIB-like asthenospheric melts (Harte 1983; Jones 1987). (Matsoku and Jagersfontein data from this study, Marid and megacryst data from Kramers *et al.* (1981, 1983).) (*b*) Melts coexisting with clinopyroxenes from basalt-derived Type II and IB xenoliths and megacrysts. (Eifel 1243 data this study, other clinopyroxene data from Wass *et al.* (1980), Irving & Frey (1984) and Menzies *et al.* (1985).) (*c*) Melts coexisting with amphibole. (The Jagersfontein, Marid and Eifel data are from this study, other source data from Irving & Frey (1984) and Menzies *et al.* (1985).)

However, the trace element abundances of melts calculated from amphibole compositions are generally lower than those calculated from clinopyroxenes, even for coexisting amphibole/clinopyroxene pairs in the same rock (e.g. Jagers 134, Eifel 1243, USA Ba172 in figure 4). The explanation is possibly that the amphibole partition coefficients used are too low by comparison with the clinopyroxene ones. Nevertheless, for our present purposes the important point is that the amphibole array of melt compositions again shows a spectrum of gradual changes such that all the melts may have arisen by differentiation processes (e.g. percolative fractional crystallization) under varying pressure–temperature conditions from a similar primitive basalt-picrite with OIB-like trace element relative abundances.

5. Discussion

The trace element data presented above support the petrographic data (§3) in their evidence for close links between dyke, vein and metasomatic rocks, and in indicating that melt differentiation processes are an important aspect of the evolution of the various dyke, vein and modal metasomatic associations. But they go beyond this to further suggest that all such associations could result from differentiation of similar primitive melts with OIB-like trace element compositions, occurring under a variety of pressure–temperature conditions.

Our major conclusion is therefore that the dykes/veins/metasomites in mantle xenoliths document processes of fractional crystallization and percolative fractional crystallization, by which primitive melts with OIB-like trace elements may differentiate to more evolved compositions, which in turn may lead to further metasomatism and enrichment in higher levels of incompatible elements. The crystallization of metasomatic and other minerals, whether it be in dykes, veins or metasomatised rocks, and their separation from the flowing/percolating melt provides the differentiation mechanism that leads to the formation of more extreme melts and their crystallization products. Thus the melts and their crystallization products evolve together, each begetting the other in the evolutionary process. This mutual relationship lies behind the conflicting arguments in the literature concerning whether metasomatism is precursory to or consequent upon magmatism (Bailey 1982; Menzies 1983; Wilshire 1987). Our thesis does not imply that the evolving melt composition eventually gives rise to the same melt (basaltic or kimberlitic) in which the mantle xenoliths are erupted; similar processes may have operated at widely separated intervals of time and thus the xenoliths may not be directly connected to the erupting melt.

Aspects of the similarities of melts/fluids involved in various types of modal metasomatism have been noted previously; e.g. Menzies *et al.* (1987) for a large set of trace element compositions, and Field *et al.* (1989) on the basis of amphibole compositions. However, unlike herein, these authors also placed emphasis on fluids distinct from melts. Menzies *et al.* (1987) considered that amphibole- and mica-rich metasomatism, particularly as represented by the richterite-bearing peridotites, was rather attributed to a hydrous fluid than a melt and emphasized low Ti characteristics as endorsing a hydrous origin. We suggest that such low-Ti characteristics may be a product of earlier and probably deeper stages of melt fractional crystallization in which abundant ilmenite is crystallized as in the Matsoku metasomites (Harte *et al.* 1987). Judging by the widespread occurrence of hydrous metasomatic phases, it is clear that the more evolved melts must be rich in H_2O, but the lack of any sharp distinction in the trace element abundance patterns of the hydrous phases contained in evolved metasomatic rocks in relation to the other assemblages (figure 4) provides no evidence for precipitation of the metasomatic phase from a separate hydrous fluid phase distinct from melt. A continuum of trace element compositions appears to exist, just as there is evidence of a continuum of petrographic characteristics (§3). This point has also been made by Kramers *et al.* (1983), and experimental data clearly support the possibility that appropriate hydrous assemblages can crystallize from a melt containing just 15% H_2O (Edgar *et al.* 1976; Waters 1987). This is not to say that a distinct hydrous phase cannot coexist with melt under appropriate circumstances, as shown by Odling & Randle (1992), but we believe that it is a differentiating melt phase which is the most likely source of the metasomatic phases.

Two other important points follow from the arguments that a spectrum of melt compositions, causing diverse aspects of modal metasomatism, can be derived by differentiation from asthenospheric melts with primitive OIB-like trace element characteristics. The first is that melts causing modal metasomatism may also be responsible for cryptic metasomatism (Dawson 1984), i.e. enrichment without modal or major-minor element change (Harte 1983, 1987). This style of metasomatism is recognized by trace element enriched (especially in LREE) compositions in clinopyroxenes in peridotites lacking petrographic evidence of metasomatism (e.g. the Type IB xenoliths from basalts, as classified by Menzies (1983)). Since the spectrum of enriched clinopyroxene compositions lies within the range of compositions seen in modal metasomatic peridotites (Neilsen & Noller 1987; Menzies *et al.* 1987) it should be possible to generate them by infiltration of the same set of melts that cause modal metasomatism. Thus they represent situations in which melt infiltrated the mantle peridotites and caused enriched trace element compositions in clinopyroxenes and other minerals, but did not cause the crystallization of any additional phases. This is fully compatible with the postulated addition of a second component to these rocks as suggested by Frey & Prinz (1978) and Frey (1980).

The second point concerns the origin of kimberlitic and lamproitic melts. Menzies *et al.* (1987), Erlank *et al.* (1987) and Waters (1987) show overlaps between the trace element compositions of kimberlites and lamproites, and various metasomatic and MARID rocks. The kimberlite/lamproite compositions fall within the compositional spectrum of melts calculated to be in equilibrium with dykes/veins/metasomites shown in figure 4. It follows that kimberlitic and lamproitic melts themselves might also be products of differentiation of primitive melts with OIB-like trace element composition, by processes of percolative fractional crystallization. In these cases, the percolation through and maintenance of local equilibrium with mantle peridotite, while undergoing crystal fractionation, is important in maintaining equilibrium with olivine and thereby ensuring the characteristic high levels of Ni in the melts. In effect the hypothesis put forward here concurs with the often-made suggestion that kimberlites are a differentiation product of the same magmas that crystallize typical megacrysts; but our proposal goes further in explaining the types of crystal fractionation and metasomatic interaction processes involved in this differentiation. However, we do not advocate that all kimberlites and lamproites arise directly by such differentiation. The differentiated liquids may well freeze in the mantle, giving rise to dykes/veins/metasomites, which upon subsequent melting, possibly much later, could form the kimberlitic and lamproitic melts (Waters 1987; McKenzie 1989). Such a two stage origin must be favoured for Group II kimberlites and those lamproites which show enriched Sr and Nd isotopic ratios. A one stage origin by differentiation from an OIB-like parent would only be appropriate for compositions like Group I kimberlites that have isotopic compositions falling within the normal mantle array indicated by basalts.

6. Conclusions

1. Surface energy considerations show that basic-ultrabasic melts should be dispersed along mineral grain edges to form a connected three-dimensional network even when present in very small volumes. This textural geometry coupled with viscosity data for the melts, indicates that very small volume melts can move through peridotitic matrices on relatively short geological timescales and enables melts to behave as metasomatic fluids.
2. Layered cumulates demonstrate the ability of basic-ultrabasic melt to flow through nearly wholly crystalline material, and precipitate mineral aggregates which do not locally represent the bulk composition of the melts.
3. The dykes, veins and modal metasomatic rocks recovered from the mantle show evidence of melt flow and accompanying crystallization processes, which leave mineral aggregates showing similarities to cumulates in textural and chemical characteristics, and which do not represent the bulk chemical composition of the

melt. The resultant rocks might be termed '*dyke cumulates*' and '*metasomatic infill cumulates*'.

4. The whole assemblage of minerals crystallized in any of the diverse and widely recognized associations of dykes, veins and modal metasomatic rocks, involves a wide array and continuum of silicate, oxide and sulphide minerals, and clearly argues for crystallization from silicate melts. No clear evidence for the operation of hydrous fluids distinct from melts has been found; with both modal mineralogical and trace element data indicating continuous ranges of compositions.

5. The formation of the various mantle dyke, veins, and metasomatic rocks demonstrates the occurrence of fractional crystallization of the melts forming them. Thus the melts undergo differentiation. These processes will often occur while the melt maintains equilibrium with the peridotitic matrix it is passing through; thus percolation (chromatographic column type) effects will also influence the evolution of melt and the term '*percolative fractional crystallization*' is suggested for this combination of processes.

6. Calculated melt compositions in equilibrium with a wide array of dyke, vein and metasomatic clinopyroxene and amphibole compositions, indicate a related progressive series of compositions which might originate by fractionation or by percolative fractional crystallization from similar asthenospherically derived primitive melts with OIB-like trace element compositions. Such melt differentiation, to varying degrees under different pressure–temperature conditions and water contents, can account for the whole array of metasomatic fluid compositions encountered in xenoliths from both basalts and kimberlites. This applies not only to modal metasomatism but also to cryptic metasomatism (where there is no modal or other petrographic expression of the passage of melt).

7. The spectrum of melt compositions generated by percolative fractional crystallization, includes ones with similar trace element compositions to kimberlites and lamproites, and thereby provides a potential means of generating such melts.

We thank colleagues in Edinburgh, particularly John Craven, Richard Hinton and Nicholas Odling for help with ion microprobe analyses and discussion of the typescript. H. Seck and G. Witt-Eickschen provided specimens of Eifel xenoliths. Mike Cheadle's wisdom on textures has been much appreciated, and he, Martin Menzies and Brian Upton kindly reviewed the typescript. Angus Miller and Gavin Andrews helped greatly with data reduction and diagram production. NERC fund the Edinburgh Ion Microprobe Facility. Assistance from De Beers Consolidated Mines Ltd with finance and rock collection has also been important.

References

Bailey, D. K. 1982 Mantle metasomatism – continuing chemical change within the Earth. *Nature, Lond.* **296**, 525–530.

Beere, W. 1975 A unifying theory of the stability of penetrating liquid phases and sintering pores. *Acta metall.* **23**, 131–138.

Bulau, J. R., Waff, H. S. & Tyburczy, J. A. 1979 Mechanical and thermodynamic constraints on fluid distribution in partial melts. *J. geophys. Res.* **84**, 6201–6108.

Bulau, J. R. 1982 Intergranular fluid distribution in olivine-liquid basalt systems. Ph.D. dissertation, Yale University, U.S.A.

Cheadle, M. J. 1989 Properties of texturally equilibrated two phase aggregates. Ph.D. thesis, University of Cambridge.

Dawson, J. B. 1984 Contrasting types of upper mantle metasomatism. In *Kimberlites. II. The mantle and crust–mantle relationships* (ed. J. Kornprobst), pp. 289–294. Amsterdam: Elsevier.

Dawson, J. B. 1987 The MARID suite of xenoliths in kimberlite: relationship to veined and metasomatised peridotite xenoliths. In *Mantle xenoliths* (ed P. H. Nixon), pp. 465–473. Chichester: Wiley.

Dawson, J. B. & Smith, J. V. 1977 The MARID (mica-amphibole-rutile-ilmenite-diopside) suite of xenoliths in kimberlite. *Geochim. cosmochim. Acta* **41**, 309–323.

Edgar, A. D., Green, D. H. & Hibberson, W. O. 1976 Experimental petrology of a highly possanic magma. *J. Petrol.* **17**, 339–356.

Eggler, D. H. 1987 Solubility of major and trace elements in mantle metasomatic fluids: experimental constraints. In *Mantle metasomatism* (ed. M. A. Menzies & C. J. Hawkesworth), pp. 21–41. London: Academic Press.

Erlank, A. J., Waters, F. G., Hawkesworth, C. J., Haggerty, S. E., Allsopp, H. L., Rickard, R. S. & Menzies, M. 1987 Evidence for mantle metasomatism in peridotite nodules from the Kimberley pipes. South Africa. In *Mantle metasomatism* (ed. M. A. Menzies & C. J. Hawkesworth), pp. 221–309. London: Academic Press.

Field, S. W., Haggerty, S. E. & Erlank, A. J. 1989 Sub-continental metasomatism in the region of Jagersfontein, South Africa. In *Kimberlites and related rocks*, vol. 2, pp. 771–783. (Special Publication no. 14). Australia: Geological Society.

Frey, F. A. 1980 The origin of pyroxenites and garnet pyroxenites from Salt Lake Crater, Oahu, Hawaii, trace element evidence. *Am. J. Sci.* A **280**, 427–449.

Frey, F. A. & Prinz, M. 1978 Ultramafic inclusions for San Carlos Arizona: petrologic and geochemical data bearing on their petrogenesis. *Earth Planet. Sci. Lett.* **38**, 129–176.

Fujii, N., Osamura, K. & Takahashi, E. 1986 Effect of water saturation on the distribution of partial melt in the olivine-pyroxene-plagioclase system. *J. geophys. Res.* **91**, 9253–9259.

Griffin, W. L., Wass, S. Y. & Hollis, J. D. 1984 Ultramafic xenoliths from Bullermerri and Grotuk Maars, Victoria, Australia; petrology of a sub-continental crust–mantle transition. *J. Petrol.* **25**, 53–87.

Gurney, J. J. & Harte, B. 1980 Chemical variations in upper mantle nodules from southern African kimberlites. *Phil. Trans. R. Soc. Lond.* A **297**, 273–293.

Haggerty, S. E. 1983 The mineral chemistry of new titanates from the Jagersfontein kimberlite, South Africa: implications for metasomatism in the upper mantle. *Geochim. cosmochim. Acta* **47**, 1833–1854.

Harte, B. 1977 Rock nomenclature with particular relation to deformation and recrystallisation textures in olivine-bearing xenoliths. *J. Geology* **85**, 279–288.

Harte, B. 1983 Mantle peridotites and processes – the kimberlite sample. In *Continental basalts and mantle xenoliths* (ed. C. J. Hawkesworth & M. J. Norry), pp. 46–91. Shiva.

Harte, B. 1987 Metasomatic events recorded in mantle xenoliths: an overview. In *Mantle xenoliths* (ed. P. H. Nixon), pp. 625–640. Chichester: Wiley.

Harte, B. & Hawkesworth, C. J. 1989 Mantle domains and mantle xenoliths. In *Kimberlites and related rocks*, vol. 2, 649–686 (Special Publication no. 14). Geological Society of Australia.

Harte, B. & Hunter, R. H. 1986 Speculations concerning the importance of metasomatic melt migration in the formation of pyroxenite sheets in garnet peridotite xenoliths from Matsoku, Lesotho. In *International Kimberlite Conference, Extended Abstracts*, pp. 184–186. Australia: Geological Society (Abstract Series no. 16).

Harte, B. & Matthews, M. B. 1989 Melt textures and ilmenite concentrations in mantle 'dykes' and metasomatic rocks. *Extended Abstracts, 28th, Int. Geol. Congress* **2**, 32–33.

Harte, B., Winterburn, P. A. & Gurney, J. J. 1987 Metasomatic phenomena in garnet peridotite facies mantle xenoliths from the Matsoku kimberlite pipe, Lesotho. In *Mantle metasomatism* (ed. M. A. Menzies & C. J. Hawkesworth), pp. 145–220. London: Academic Press.

Harte, B., Pattison, D. R. M. & Linklater, C. M. 1991*a* Field relations and petrography of partially melted pelitic and semi-pelitic rocks. In *Equilibrium and kinetics in contact metamorphism* (ed. G. Voll, J. Topel, D. R. M. Pattison & F. Seifert), pp. 181–209. Berlin: Springer-Verlag.

Harte, B., Matthews, M. B., Winterburn, P. A. & Gurney, J. J. 1991*b* Aspects of melt composition, crystallization, metasomatism and distribution, shown by mantle xenoliths from the Matsoku Kimberlite pipe. In *Fifth International Kimberlite Conference Extended Abstracts: CPRM* (*Special Publication* 2/19, pp. 167–169. Brasilia.

Hofmann, W. W. 1972 Chromatographic theory of infiltration metasomatism and its application to feldspars. *Am. J. Sci.* **272**, 69–90.

Hunter, R. H. 1987 Textural equilibrium in layered igneous rocks. In *Origins of igneous layering* (ed. I. Parsons), pp. 473–503. D. Reidel.

Hunter, R. H. & McKenzie, D. 1989 The equilibrium geometry of carbonate melts in rocks of mantle composition. *Earth planet. Sci. Lett.* **92**, 347–356.

Irving, A. J. 1980 Petrology and geochemistry of composite ultramafic xenoliths in alkalic basalts and implications for magmatic processes within the mantle. *Am. J. Sci.* A **280**, 389–426.

Irving, A. J. & Frey, F. A. 1984 Trace element abundances in megacrysts and their host basalts: constraints on partition coefficient and megacryst genesis. *Geochim. cosmochim. Acta* **48**, 1201–1221.

Jones, R. A. 1987 Strontium and neodymium isotopic and rare earth element evidence for the genesis of megacrysts in kimberlites of southern Africa. In *Mantle xenoliths* (ed. P. H. Nixon), pp. 711–724. Chichester: Wiley.

Jones, A. P., Smith, J. V. & Dawson, J. B. 1982 Mantle metasomatism in 14 veined peridotites from Bultfontein mine, South Africa. *J. Geology* **90**, 435–453.

Jurewicz, S. R. & Jurewicz, A. J. G. 1986 Distribution of apparent angles on random sections with emphasis on dihedral angle measurements. *J. geophys. Res.* **91**, 9277–9282.

Jurewicz, S. R. & Watson, E. B. 1985 Distribution of partial melts in granitic system: the application of liquid phase sintering. *Geochim. cosmochim. Acta* **49**, 1109–1121.

Kingery, W. D., Bowen, H. K. & Uhlmann, D. R. 1976 *Introduction to ceramics*. New York: Wiley Interscience.

Kramers, J. D., Smith, C. B., Lock, N. P., Harmon, R. S. & Boyd, F. R. 1981 Can kimberlites be generated from an ordinary mantle. *Nature, Lond.* **291**, 53–56.

Kramers, J. D., Roddick, J. C. M. & Dawson, J. B. 1983 Trace element and isotopic studies on veined, metasomatic and 'MARID' xenoliths from Bultfontein, South Africa. *Earth planet. Sci. Lett.* **65**, 90–106.

Laporte, D. 1988 Wetting angle between silicic melts and biotite (abstract). *Eos, Wash.* **69**, 1411.

Lloyd, F. E. 1987 Characterization of mantle metasomatic fluids in spinel cherzolites and alkali clinopyroxenites from the west Eifel and south west Uganda. In *Mantle metasomatism* (ed. M. A. Menzies & C. J. Hawkesworth), pp. 91–123. London: Academic Press.

Matthews, M. B. & Harte, B. 1989 Preservation of melt textures in mantle xenoliths. *Terra Abstr.* **1**, 274.

Matthews, M., Harte, B. & Prior, D. 1992 Mantle garnets: a cracking yarn. *Geochim. cosmochim. Acta* **56**, 2633–2642.

McKenzie, D. P. 1984 The generation and compaction of partially molten rock. *J. Petrol.* **25**, 713–765.

McKenzie, D. 1989 Some remarks on the movement of small melt fractions in the mantle. *Earth planet. Sci. Lett.* **95**, 53–72.

McKenzie, D. & O'Nions, R. K. 1991 Partial melt distributions from inversion of rare earth concentrations. *J. Petrol.* **32**, 1021–1091.

Menzies, M. A. 1983 Mantle ultramafic xenoliths in alkaline magmas: evidence for mantle heterogeneity modified by magmatic activity In *Continental basalts and mantle xenoliths* (ed. C. J. Hawkesworth & M. J. Norry), pp. 92–110, Shiva: Nantwich.

Menzies, M. A., Kempton, P. & Dungon, M. 1985 Interaction of continental lithosphere and asthenosphere melts below the Geronimo volcanic field. Arizona, U.S.A. *J. Petrol.* **26**, 663–693.

Menzies, M. A., Rogers, N., Tindle, A. & Hawkesworth, C. J. 1987 Metasomatic and enrichment processes in lithospheric peridolites, an affect of asthenosphere–lithosphere interaction. In *Mantle metasomatism* (ed. M. Menzies & C. J. Hawkesworth), pp. 313–361. London: Academic Press.

Navon, O. & Stolper, E. 1987 Geochemical consequences of melt percolation: the upper mantle as a chromatographic column. *J. Geology* **95**, 285–307.

Nicholas, A. 1986 A melt extraction model based on structural studies in mantle peridotites. *J. Petrol.* **27**, 999–1022.

Nicholas, A. & Jackson, M. 1982 High temperature dikes in peridolites: origin by hydraulic fracturing. *J. Petrol.* **23**, 568–582.

Nielson, J. E. & Noller, J. S. 1987 Processes of mantle metasomatism; constraints from observations of composite peridotite xenoliths. *Geol. Soc. Am. Spec. Pap.* **215**, 61–76.

Odling, N. W. A. & Randle, H. A. 1992 The partitioning of trace elements between fluid and melt. *Terra Nova (abstracts)* **4**, 32–33.

O'Nions, R. K. & McKenzie, D. P. 1988 Melting and continent generation. *Earth planet. Sci. Lett.* **90**, 449–456.

Riley, G. N. & Kohlstedt, D. L. 1991 Kinetics of melt migration in upper mantle rocks. *Earth planet. Sci. Lett.* **105**, 500–521.

Smith, C. S. 1948 Grains phases and interfaces: an interpretation of microstructure. *Trans AIME* **197**, 15–51.

Sun, S.-S. & MacDonough, W. F. 1989 Chemical and isotopic systematics of ocean basalts; implications for mantle composition and processes. In *Magmatism in the ocean basins* (ed. A. D. Saunders & M. J. Norry), pp. 313–345. *Geol. Soc. Lond. Spec. Publ.* **42**.

Toramaru, A. & Fujii, N. 1986 Connectivity of a melt phase in a partially molten peridotite. *J. geophys. Res.* **91**, 9239–9252.

Vincenzi, E. P., Rapp, R. & Watson, E. B. 1988 Crystal/melt wetting characteristics in partially molten amphibolite (abstract). *Eos, Wash.* **69**, 482.

Voll, G. 1960 New work on petrofabrics. *Liverp. Manch. Geol. J.* **1**, 73–85.

Von Bargen, N. & Waff, H. S. 1988 Wetting of enstatite by basaltic melt at 1350 °C and 1.0–2.5 GPa pressure. *J. geophys. Res.* **93**, 1153–1158.

Waff, H. S. & Bulau, J. R. 1979 Equilibrium fluid distribution in an ultramafic partial melt under hydrostatic stress conditions. *J. geophys. Res.* **84**, 6109–6114.

Wager, L. R., Brown, G. M. & Wadsworth, W. J. 1960 Types of igneous cumulates. *J. Petrol.* **1**, 73–85.

Walker, D., Jurewicz, S. & Watson, E. B. 1988 Adcumulus dunite growth in a laboratory thermal gradient. *Contrib. Mineral. Petrol.* **99**, 306–319.

Wass, S. Y., Henderson, P. & Elliot, C. J. 1980 Chemical heterogeneity and metasomatism in the upper mantle: evidence from rare earth and other elements in apatite rich xenoliths in basaltic rocks from eastern Australia. *Phil. Trans. R. Soc. Lond.* A **297**, 333–346.

Waters, F. G. 1987 A suggested origin of MARID xenoliths in kimberlites by high pressure crystallisation of an ultrapotassic rock such as lamproite. *Contrib. Miner. Petrol.* **95**, 523–533.

Watson, E. B. & Brenan, J. M. 1987 Fluids in the lithosphere. I. Experimentally determined wetting characteristics of CO_2–H_2O fluids and their implications for fluid transport, host-rock physical properties and fluid inclusion formation. *Earth planet. Sci. Lett.* **85**, 497–515.

Wilshire, H. G. 1987 A model of mantle metasomatism. *Geol. Soc. Am. Spec. Vol.* **215**, 47–60.

Wilshire, H. G. & Pike, J. E. N. 1975 Upper mantle diapirism: evidence from analogous features in alpine peridotite and ultramafic inclusions in basalt. *Geology* **3**, 467–470.

Wilshire, H. G. & Shervais, J. W. 1975 Al augite and Cr diopside ultramafic xenoliths in basaltic rocks from the western United States. *Phys. Chem. Earth* **9**, 257–272.

Wilshire, H. G. & Trask, N. J. 1971 Structural and textural relationships of amphibole and phlogopite in peridotite inclusions, Dish Hill, California. *Am. Mineralogist* **56**, 240–251.

Wilshire, H. G., Pike, J. E. N., Meyer, C. E. & Schwarzmann, E. C. 1980 Amphibole-rich veins in lherzolite xenoliths, Dish Hill and Deadman Lake, California. *Am. J. Sci.* A **280**, 576–593.

Witt, G. & Seck, H. A. 1987 Temperature history of sheared mantle xenoliths from west Eifel, west Germany: evidence for mantle diapirism beneath the Rhenish Massif. *J. Petrol.* **28**, 475–494.

Winterburn, P. A., Harte, B. & Gurney, J. J. 1990 Peridotite xenoliths from the Jagersfontein kimberlite pipe. I. Primary and primary-metasomatic mineralogy. *Geochim. cosmochim. Acta* **54**, 329–341.

Wyatt, B. A. & Lawless, P. J. 1984 Ilmenite in polymict xenoliths from the Bultfontein and De Beers mines, South Africa. In *Kimberlites II: the mantle and crust–mantle relationships* (ed. J. Kornprobst), pp. 43–56. Amsterdam: Elsevier.